

Intermixing and Diffusion Impact on CdS/CdTe/p⁺ Regions (Te or ZnTe)/Cu/Au Solar Cell Interphases

C. Hernández-Vásquez^{a*} , M.L. Albor-Aguilera^b , J.M. Flores-Marquez^c ,
M.A. González-Trujillo^a 

^aInstituto Politécnico Nacional, CDMX, 07738, Ciudad de México, México.

^bInstituto Politécnico Nacional, Departamento de Física, CDMX, 07738, Ciudad de México, México.

^cInstituto Politécnico Nacional, Departamento de Ingeniería en Metalurgia y Materiales, CDMX, 07738, Ciudad de México, México.

Received: November 08, 2022; Revised: May 02, 2023; Accepted: May 30, 2023

The polycrystalline CdS/CdTe thin film solar cell is one of the most important photovoltaic devices for cost-effective generation of solar electricity for terrestrial applications. A typical superstrate structure of CdTe solar cell has been studied through current-voltage (J-V) and secondary ion mass spectroscopy (SIMS) measurements. A close correlation between quality of interphases and its photovoltaic efficiency was determined. It was found an improvement of open circuit voltage (V_{oc}) and efficiency associated to CdS and CdTe thermal treatments, and a reduction of diffusion of S and Cd into CdTe and CdS respectively. An efficiency of 12% has been reached on solar cells with a Te and ZnTe interlayer as part of the back contact. Low diffusion of Cu along absorbent material was observed when Te and ZnTe was used creating a stable back contact along the time. Diffusion and intermixing at each junction SnO₂:F/CdS, CdS/CdTe and CdTe/Te or ZnTe/Cu/Au was found, establishing limit values of element diffusion along CdTe solar cells.

Keywords: CdTe, Solar cells, Depth profile, photovoltaic efficiency, Diffusion, Intermixing, p⁺ regions.

1. Introduction

The photovoltaic trade has been dominated by crystalline silicon technology, which requires high-energy intensive processes. On the opposite side, thin film technology employs deposition methods as simple as possible, low production costs and high efficiencies. However, the efficiency of PV devices is mainly influenced by charge transport across the heterojunction formed by both materials: the window and absorber material. So, the materials for photovoltaic conversion could be selected considering the follow characteristics as highly desired: a direct band gap with values near to the visible light spectrum; and a high optical absorption coefficient.

1.1. Window material and chemical bath deposition (CBD) method

Chemical Bath Deposition (CBD) has proven to be the best technology for CdS production due to it provides a variety of routes to produce a functional film at relative low temperatures by immersing a substrate in a chemical solution^{1,2} allowing scale-up technological process for larger deposition areas at lowest cost. CdS as window material must be free of defects such as inter grain caves and pin-holes. The CdS has a band gap value around 2.4 eV that causes absorption of photo-generated carries in the short wavelength region. The reduction of CdS thickness layer could improve the short-circuit current density and blue response together Fluorine Tin Oxide (FTO)^{3,4}.

1.2. Absorber material and deposition method: CdTe by CSVT

The II-VI heterostructures based solar cells like CdTe ones, are promising candidates because of its low cost and high photovoltaic efficiency devices. The highest reported efficiencies are not still near to the theoretical limits (18 – 24%)⁵. The CdTe semiconductor material has been used in photovoltaic devices as absorbent material, CdTe has a band gap value of 1.5 eV, and it was obtained by different techniques that allows get specific properties. Techniques such as magnetron sputtering could fabricate ultra-thin CdTe layer with crystallographic texture and thickness around 0.5 and 1.28 μm ⁶, laser ablation technique allows to obtain nanoparticles of CdTe and thin films around 1.8 and 3 μm with two different crystalline structures (cubic and hexagonal)^{7,8}, spray pyrolysis technique has been used to growth CdTe thin films from an aqueous colloidal dispersion of CdTe obtaining a crack-free CdTe⁹, electrodeposition technique is a viable technique to deposited thin films due to simplicity, CdTe thin films was deposited on flexible substrate obtaining grain size around 500 nm as is reported by Mathew et al.¹⁰, and close space vapor transport (CSVT) equipment that allows created CdTe thin films with adequate structural, optical, electrical properties^{11,12}. Important characteristics are demanding for CdTe films; stoichiometry, growth morphology, adequate crystalline structure; in particular, CdTe growth with preferential phase on (111) plane¹³.

*e-mail: chernandezex@gmail.com

Additionally, a thermal annealing of CdTe thin films by CdCl₂ plays an important role in the photovoltaic process; it increases the CdTe grain size and reduce the grain boundary¹⁴⁻¹⁶. The record efficiency into CdS/CdTe solar cells are 21.3% at laboratory level and 16% at commercial solar panels¹⁷. These efficiencies, however, are well below of the theoretical limit of about 30% calculated by Schockley and Queisser¹⁸.

On the other hand, it is important to remark that the transport could be strongly influenced by the quality of the interphases during solar cell fabrication. In order to achieve this the intermixing and diffusion are study on each step process of CdTe solar cell by SIMS, SEM, EDS. Analyzing the diffusion of elements that constitute the window material, absorbent material, thermal treatments, and p⁺ regions (Te or ZnTe) the last ones have been proposed as interlayer between the CdTe film surface and the metallic layer. These regions allowed to get a smoothed CdTe surface and consequently a better alignment of the bands that clearly reduced the potential barriers¹⁹. Bätzner et al.²⁰ different etching treatments process produce a conducting Te layer that allow get stable and non-rectifying back contact. On another hand ZnTe regions has been implemented resulting in an improvement on open circuit voltage and efficiency using 300nm of thickness²¹; Zn accumulation has been detected at the edge of Cu_xTe cluster that are former after ZnTe deposition on CdTe²² and efficiencies about 15% has been reached using ZnTe films around 35nm²³. However, at the back contact is important determine what are the principal problematics on the solar cells conformation. Finally different solar cells devices were developed to understand the electrical behavior of each solar cell considering the intermixing and diffusion along the solar cell.

2. Experimental Details

2.1. Thin films growth

CdTe solar cells were grown in a superstrate configurations onto commercial SnO₂:F substrates (FTO). CdS thin films were grown by CBD on FTO substrates treated chemically on HCl, as a precursor solution were used NH₄Cl (0.2 M), CdCl₂ (0.12 M), NH₃ (2M) and (NH₂)₂CS (0.3M) at temperature of 70°C for 4 min. All samples were thermally treated in air (TT_{air}) at 450 °C for 60 min.

CdS films shown thickness about 60 nm and 85% of transmittance with a band gap value of 2.42 eV²⁴. The CdTe films were deposited on CdS thin films by using CSVT equipment. CdTe source powder Sigma Aldrich® with a purity of 99.99% (0.0130g ± 0.0005g) was set up in evaporation chamber (see Figure 1). A thermal gradient between source and substrate blocks of 100 °C was used, the vacuum degree for the deposition process is 10⁻¹Torr considering an atmosphere of 50% Argon (Ar) and 50% Oxygen (O₂) atmosphere was used by 3min (deposition time). The CdTe thickness layer was around 3 μm. CdTe films were thermally treated with CdCl₂ (TT_{CdCl2}) and Ar atmosphere during 3 min on CSVT system, after that samples were cleaned with distilled water to remove remnants of CdCl₂ grains and dry with Nitrogen (N₂) gas. The CdS/CdTe junction was activated by thermal treatment in air at 450°C for 30 min. After that to enhancement CdTe solar cells and study the effect of p⁺ regions Tellurium (Te) and Zinc-Tellurium (ZnTe) were deposited on different samples. To deposited Te, a compound is collocated on a graphite container into CSVT system using a substrate temperature of 300°C by 30 min (see Figure 1), it allows get a nanostructured region on CdTe, additionally a thermal treatment is done by 20 min on air to recrystallize this region. On the other hand, a ZnTe region is deposited on CdTe using an inert atmosphere (Ar) during 3 and 5 min using a temperature gradient of 500°C and 700°C respectively. Finally, standard back contacts consist of an evaporated Cooper (Cu) / Gold (Au) layer^{25,26}.

Layer thicknesses were measured with a step profiler (Sloan Dektak II). The morphology of the surface samples was analyzed by a scanning electron microscope (SEM) JEOL series JSM7X and elemental analysis EDS was obtained using an EDAX detector with a spectral resolution of 129 eV and 0.001 cps/eV using an acceleration voltage of 10 kV. K-line and L-line were used to detect (Cd, Te, Cl, S, Sn and O). APB-ZAF correction method was applied. In order to investigate the abruptness of the interphases generated, secondary ion mass spectroscopy (SIMS) depth profiling were performed by using an IONTOF 5 spectrometer; the measurements were obtained by using liquid bismuth source at 30 keV for analysis and Cesium beam at 1 keV for sputtering. Considering an incidence beam at 45 nominal degrees. Craters of 400 μm² were eroded but only 200 μm² were considered for analyses; this one to exclude boarder effects on measurements.

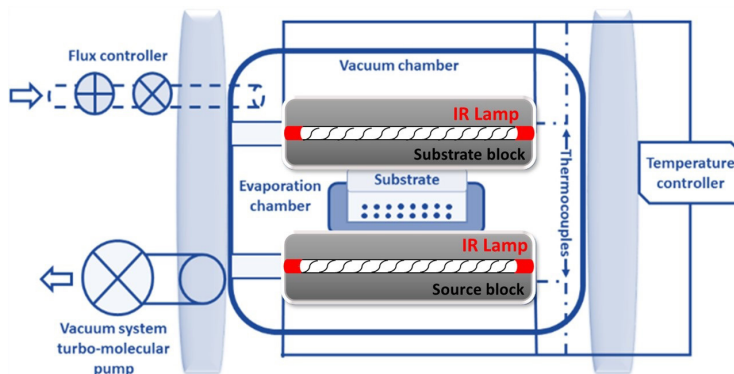


Figure 1. Schematic diagram of CSVT system used to growth and thermal treatments.

2.2. CdTe solar cells

CdTe solar cells has been developed along time, and different analysis were made to understand the behavior of each material in this kind of devices. This work establishes an understanding about intermixing or diffusion between interphases by SIMS and SEM. Five prototypes solar cells were considered for this purpose as is observed in Table 1.

CdTe solar cell structure is showed in Figure 2a. These solar cells were developed as is detailed in Figure 2b to analyze each step of the process (window material, absorbent material, back contacts). I-V measurements were obtained with a (Sol3A Class AAA Solar simulator IEC/JIS/ASTM, 1000 Watt Xenon) equipment with a light source of ($100\text{mW}/\text{cm}^2 - \text{AM1.5}$) and a QEPVSI-b Oriol Instrument was used to obtain the spectral response and quantum efficiency values.

3. Results and Discussion

3.1. Intermixing and diffusion analysis in thin films layers at intermediated steps

Trial structures based on CdS/CdTe were fabricated using all the different protocols above describe. Quantitative SIMS and qualitative SEM/EDS was used to check the incorporation of elements into the films along the complete solar cells, checking each step process as is mentioned in the following sections to determine the influence and impact on electrical behavior.

Table 1. CdTe solar cells structures designed to analyze the diffusion and intermixing of elements present along the device.

Nomenclature	Solar Cell Structure
P1	FTO/CdS/CdTe/Cu/Au
P2	FTO/CdS+TT _{air} /CdTe/Cu/Au
P3	FTO/CdS+TT _{air} /CdTe+TT _{CdCl2} /Cu/Au
P4	FTO/CdS+TT _{air} /CdTe+TT _{CdCl2} /Te/Cu/Au
P5	FTO/CdS+TT _{air} /CdTe+TT _{CdCl2} /ZnTe 700°C by 3 min/Cu/Au

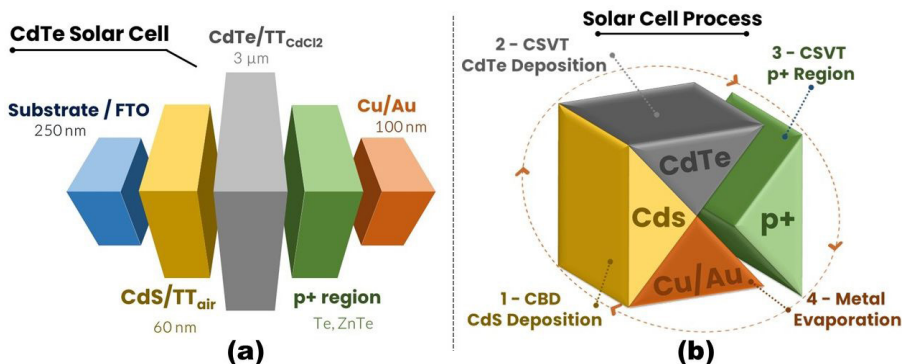


Figure 2. a) CdTe solar cell structure, b) CdTe solar cell process

3.1.1. Window material ($\text{SnO}_2:\text{F}/\text{HCl}/\text{CdS}$) step

CdS thin films were deposited by CBD onto $\text{SnO}_2:\text{F}$ (FTO) substrates previously treated with HCl ¹, CdS thin film shows a conglomerates structure (see Figure 3a), producing a softly material that can be used as window material due to it could be sublimated with CdTe sublimation temperature without affecting performance on photovoltaic device. However, SIMS measurement allows analyze intermixing and diffusion of each element that conforms these thin films. In this way from Figure 3b, is possible to observe a Sulfur (S) diffusion about 22.5nm, Cadmium (Cd) diffusion around of 13.6nm and finally a Chlorine (Cl) diffusion or remanent is detected from HCl chemical treatment along FTO; after the CdS films was thermal annealed in air at 450°C for 60 min., CdO crystals appear on surface with the thermal treatment; This thermal treatment produces a phase transition from CdS to CdO changing the optical band²⁷. It could be associated to the increase of O_2 concentration in the CdS thin films producing a decrease of the crystallinity, then the band gap contribution of CdO allow to use more photon of solar radiation. Figure 3c as shows in SEM image of CdS surface where CdO crystals appear clearly along CdS surface. An elemental quantification of Cd and S atomic percent was made, obtaining 64% and 36% atoms respectively. Figure 3d shows a depth profile considering Cd, S, Cl and O signals along the FTO/CdS; where S diffuses into FTO around 42nm, Cd diffuses 153.4nm and Cl diffuses completely in FTO without reach substrate. Diffusion of Cd, S and Cl has a close correlation with its ionic radii. Cd ionic radii (0.97 \AA) is small when it works with +2, S ionic radii (1.84 \AA) is bigger when works with -2, it diffuses to FTO like Cd, when CdS thin film is thermally treated, but much less than Cd. Cl approach size of S when it works with -1, around of 1.81 \AA , however, if Cl_2 is molecular, it has a covalent bond and its radii is about 0.99 \AA , which would explain why it diffuses as much as Cd to the FTO when thermal treatment is performed, at the same time Cl was detected in the CdS due to it escape to the atmosphere considering that Cl comes from precursor solutions and chemical activation done to FTO. On the other hand, a less signal due to O that appears on FTO and CdS surface, this signal could be associated with CdO crystals. Thermal treatment on CdS increase diffusion of S and Cd on FTO creating a better match between CdS and $\text{SnO}_2:\text{F}$ increasing the J_{sc} and R_{sh} on CdTe solar cells as is observed on CdTe solar cells electrical parameters.

3.1.2. Absorbent material ($\text{SnO}_2\text{:F/HCl/CdS/CdTe}$) step

Figure 4a shows CdTe polycrystalline as grown on CdS films; an elemental analysis reveals an atomic percentage of Cd and Te around 43% and 57% respectively; due Cd vacancies, the CdTe is p-type. CdTe grains have average size of 4 μm and they are characterized by a twin conformation. XRD patterns of as deposit CdTe show a (111) orientation. Depth profile in Figure 4b shows a CdTe region conformed by uniform Cd and Te signals; S signal is confined on CdS region, nevertheless, a low diffusion (180nm) on CdTe thin film is determine, in the same way Te signal is detected on CdS thin films diffusing 270nm reaching FTO, the diffusion between CdS and CdTe can be reduced due to CdO crystals. As is reported for different researchers the $\text{CdS}_x\text{Te}_{1-x}$ could be created^{28,29}. Figure 4c show a SEM image of CdTe thermally treated with CdCl_2 by CSVT, some crystals of CdCl_2 appear on CdTe surface and the CdTe twins are reduced; Elemental analysis reveals for recrystallized CdTe films an atomic percent of 49%, 47% and 4% of Cd, Te and Cl respectively;

comparing this data with not recrystallized CdTe samples, the quantity of Cd atoms increase on 8% and Te atoms are reduced on 18%. This treatment produces a blue surface associated to the CdTe grains orientation and CdCl_2 grains at the CdTe surface, and it can assure a good response in the solar cells³⁰. Figure 4d shows a depth profile, where S and Te diffusion increase on CdTe and CdS thin films around 230nm and 400nm respectively. A comparison between CdTe as grown and CdTe thermally treated structures, can show EQE spectra from 550 nm to 800 nm where more photons are absorbed in this range, more electron hole pairs are also generated in this range. Hence more carriers contribute to current. Furthermore, the Cl trace appears along the CdTe bulk, with major intensity at CdTe bulk (see Figure 4d) increasing diffusion to 1.56 μm . As part of the CdTe solar cells process a finally thermal treatment on air is made and a rinsed process is made to the CdTe surface treated with distilled water to reduce CdCl_2 grains (see Figure 4c). It promotes a reduction of Cl signal along to the CdTe bulk (see Figure 4d).

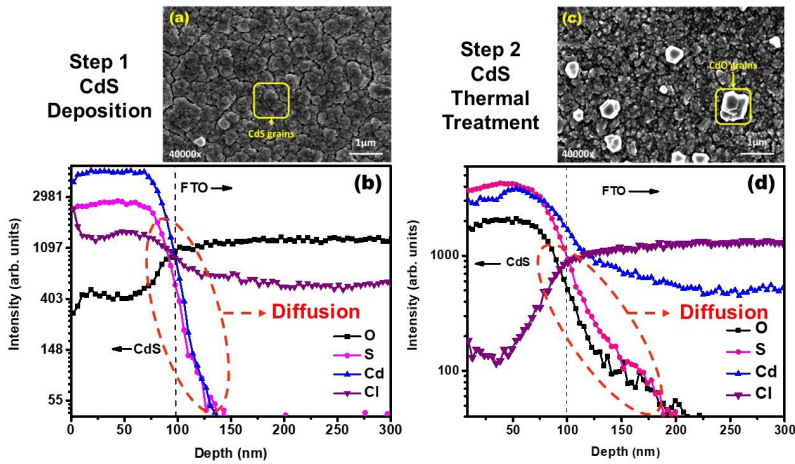


Figure 3. SEM images at 5kV of (a) CdS thin film deposited on FTO substrate and (c) CdO crystals distribution along CdS thin film, depth profile by SIMS of (b) FTO/ CdS, and (d) FTO/ CdS+TT_{air}

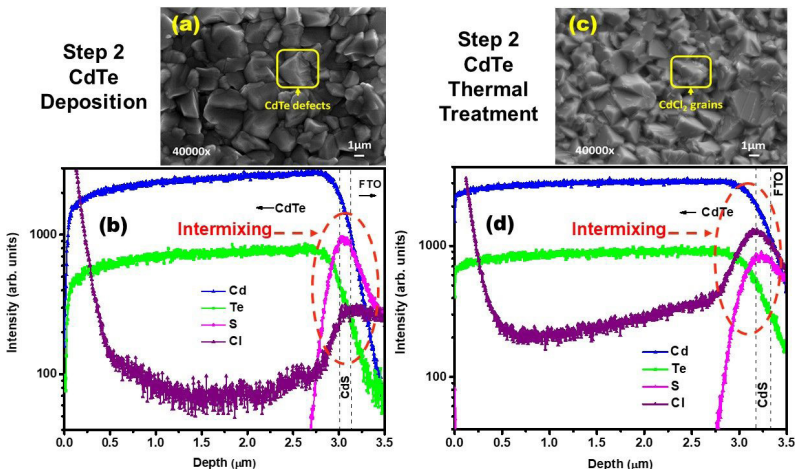


Figure 4. SEM images at 5 kV and SIMS results of CdTe (a) as grown, (c) recrystallized CdTe film, depth profile by SIMS of (b) CdTe as grown, (d) recrystallized CdTe film.

3.1.3. Back contacts ($\text{SnO}_2\text{:F/HCl/CdTe/Te}$ or ZnTe) step

3.1.3.1. Te region

An alternative model for glass/FTO/CdS/CdTe/metal solar cells is formulate, due to commonly electrical resistivity values for CdTe are found in $10^6 \Omega \cdot \text{cm}$ range, consequently CdTe/metal is not a good Ohmic junction. In this way a nanostructured Te region on CdTe surface is deposited (see Figure 5a); Elemental analysis shows values of 45% and 55% of Cd and Te respectively considering the bulk interaction, at the same time electrical measurements were improved on CdTe surface with the Te region from $10^6 \Omega \cdot \text{cm}$ to $10^2 \Omega \cdot \text{cm}$. Considering that parallel high conductivity paths (shunts) across the CdTe solar cell p-n junction or on the cell-edges are related to shunt resistance. Some paths give rise to the shunt current such as impurities in and near the junction, presence of different defects, crystal scratches and manufacturing process. Shunt paths lead the current away from the intentional load, and their effects are detrimental to the module performance mainly at low intensity levels. In this way optimization of contacts and contact resistances will add more complexity to the analysis, a simple ohmic contact with negligible resistance is considered assume when resistivity of the material is reduced due to an ohmic contact with no resistance create a better

performance on solar cell, then these results allow improving the ohmic properties on CdTe/metal junction, increasing shunt resistance and create a better CdS/CdTe junction, it could be observed on J-V curves and EQ spectra. In Figure 5c SEM image allows to observed the Cu/Au metal contacts on CdTe grains, and Figure 5d shows the depth profile of CdTe solar cell, the Au, Cu, Cd and Te elements ratio compared with Cu quantity on metal/semiconductor junction was analyzed. The depth profile was analyzed in the region, from 0 nm to 0.5 μm . Cu and Au has problems in different ways, mainly is migration, however, using the Te region on CdTe was possible to observed how it stops. Analyzing the depth resolution $\Delta z_{\text{diffusion}}$ between 16% and 84% on the graphs. The structure shows a $\Delta z_{\text{diffusion}}(\text{Cu}) = 138 \text{nm}$ in Cd, a $\Delta z_{\text{diffusion}}(\text{Cu}) = 117 \text{nm}$ in Te, on the other hand the device shows a $\Delta z_{\text{diffusion}}(\text{Au}) = 150 \text{nm}$ in Cd, a $\Delta z_{\text{diffusion}}(\text{Au}) = 100 \text{nm}$ in Te, considering the edge in Cd and Te signals, as it is observed the diffusion is reduced into CdTe thin films.

Figure 6 shows a cross sectional SEM image and lineal EDS for $\text{SnO}_2\text{:F/HCl/CdTe/Te}$ structure. The CdS/FTO junction can be distinguish clearly, besides it, lineal EDS allow to observed a Sn signal from $\text{SnO}_2\text{:F}$ thin films and Cd peak from CdS thin films. CdTe region exhibits its typically twins grains conformation, with a uniform Cd and Te signals along solar cells.

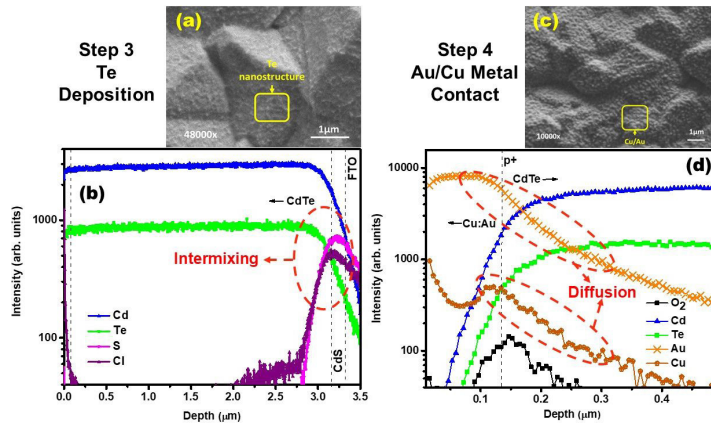


Figure 5. SEM images at 5kV of (a) Te deposition, and (c) Cu/Au Metals deposition, depth profile by SIMS for (b) $\text{SnO}_2\text{:F/HCl/CdTe/Te}$ structure and (d) $\text{SnO}_2\text{:F/HCl/CdTe/Te/Cu/Au}$ structure.

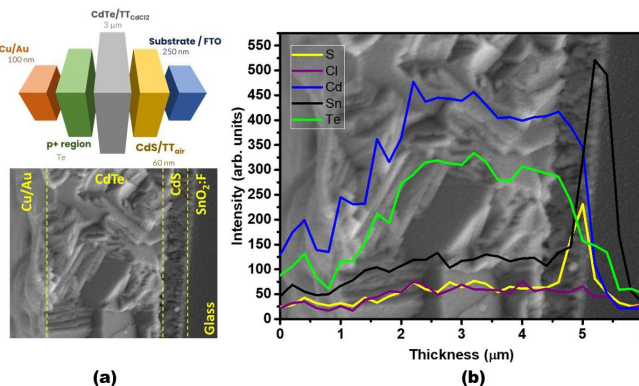


Figure 6. $\text{SnO}_2\text{:F/HCl/CdTe/Te}$ structure analyzed by (a) Cross sectional SEM and (b) lineal EDS.

Additionally, O and Cl signals is observed through complete device, it can be explained in different ways, the most representative behaviors are related to Cl on CdTe grains boundaries, considering that Cl signal comes from chemical treatment to FTO, precursors solutions associated to CdS deposition and the thermal treatment on CdCl₂ to CdTe surface; Additionally O is associated to CdS surface oxidation³¹⁻³³ and formation of TeO₂ on CdTe surface³⁴. As we can see in Figure 6 the cross-sectional SEM image of CdTe/CdS interfaces are not abrupt due to a changing hetero-interface structure decreases the lattice mismatch, and CdS/CdTe interface could be modified into CdS/CdO/CdTe or CdS/CdS_{1-x}Te_x/CdTe ternary phase according to the sulfur diffusion along CdTe and CdO crystals present on CdS surface (see Figure 4d and Figure 5b). The formation of ternary compounds is related to the growth temperature of CdTe. On another hand the Cd diffusion into CdTe is stopped by oxygen atoms present on CdS surface.

Finally, a good uniform deposition of Cu and Au on Te/CdTe grains is appreciate.

3.1.3.2. ZnTe region

The ZnTe regions obtained were slightly grey along the complete CdTe surface, uniform ZnTe deposition on CdTe surface for 500°C by 3 and 5 min and 700°C for 3 min, however, it is not uniform for 700°C by 5 min, with smooth surface characteristic to ZnTe. The surface SEM images of films deposited at different temperatures and times are given in Figure 7a, 7c, 7e. The SEM images show that films are homogenous in CdTe surface. A granular morphology is observed for 500°C by 3 and 5 min and a columnar morphology can be observed for 700°C by 3 min. Allowing identify grain boundaries associated to CdTe grains. The thickness of the films is homogenous and continuous throughout the whole length of the films, although ZnTe deposited by 5 min at 700°C create a thin film on CdTe surface vanishing the grain boundaries.

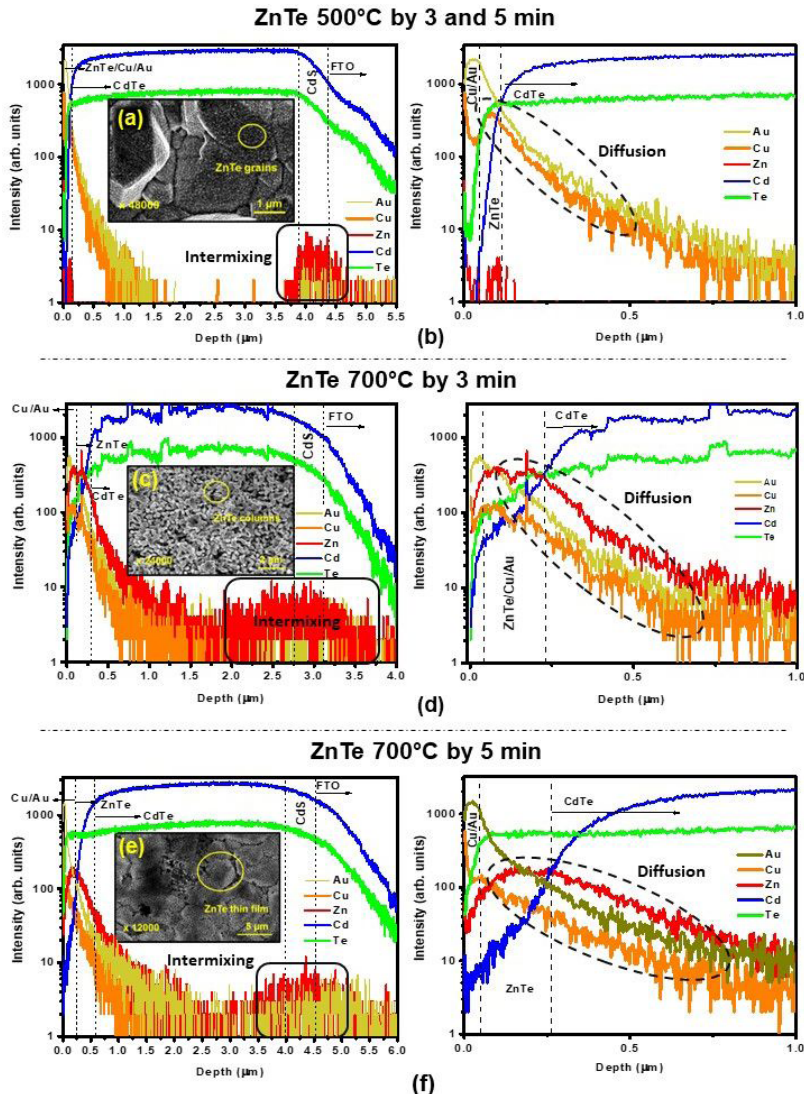


Figure 7. SEM images of ZnTe deposited on CdTe surface at 500°C by (a) 3 min and 5 min and 700°C by (c) 3 min and (e) 5 min, SIMS depth profiles of samples with ZnTe at (b) 500°C by 3 and 5 min, (d) 700°C by 3 min and (f) 700°C by 5 min.

To analyze the behavior of Zn and Te elements along CdTe, SIMS measurements were performed. In Figure 7b, 7d, and 7f depth analysis was performed, it is observed the intermixing and diffusion of each element along CdS/CdTe structure, at the same time Cu and Au was analyzed. Leading and trailing edges of a measured delta distribution allow to understand the possible diffusion along the thin films³⁵, in order to check it and comparing diffusion on each step graphs in Figure 7b shows a diffusion of Cu and Au into CdTe/ZnTe (500°C by 3 and 5 min); a maximum diffusion for $Au_{diffusion} = 265.8nm$ and $Cu_{diffusion} = 263.5nm$ is obtained under these conditions and a lower diffusion is about of $Au_{diffusion} = 94.3nm$ and $Cu_{diffusion} = 100.6nm$, considering an average thickness of ZnTe thin film around of 91nm, however, a zinc signal is not appreciated in CdTe region. In Figure 7d is showed a depth profile of ZnTe deposited on CdTe surface by 700°C for 3 min, diffusion of Cu and Au is analyzed too, getting a maximum diffusion of $Au_{diffusion} = 428.7nm$ and $Cu_{diffusion} = 488.1nm$, while the lower diffusion for Cu and Au are $Au_{diffusion} = 194.4nm$ and $Cu_{diffusion} = 202.6nm$, the last results are considering a thickness of ZnTe deposition around 187.9nm; according to ZnTe deposition on CdTe surface a Zn signal is observed in Figure 7d, showing a diffusion from 11.6nm up to 228.8nm. Finally in Figure 7f is showed a depth profile of CdS/CdTe/ZnTe structure where ZnTe was deposited at 700°C by 5 min. The maximum and minimum diffusion of Cu and Au in this structure are $Au_{diffusion} = 634nm$, $Au_{diffusion} = 240.7nm$ and $Cu_{diffusion} = 696nm$ and $Cu_{diffusion} = 252.7nm$ respectively, considering an average thickness of ZnTe about 212.1nm. In concordance with Figure 7f a Zn signal is observed along CdTe, the maximum and minimum diffusion are $Zn_{diffusion} = 679.3nm$ and $Zn_{diffusion} = 245.5nm$ respectively. As a consequence of

these results, we could observe that temperature impact the diffusion of Cu and Au along CdTe/ZnTe structure. In Figure 7b, 7d, and 7f the Zn signal reaches CdS/CdTe junction, probably it produces a bad function of solar cells, due to electrical carriers can found a short route between both contacts and could generate a short circuit in the device or an increase on current. The last results allow to identify an increment on ZnTe thickness; however this produces a thin film on CdTe surface reducing the large grain boundaries associated to CdTe, it means create more potential barriers limiting the flux of carriers to the back contact, in this way the best option is create grains that has a preferential direction. In order to identify the impact and effect of each element along the solar cell structures analyzed before some solar cells were developed to determine the influence of these.

3.1.4. CdTe solar cells performance

Figure 8a, 8b shows I-V and J-V curves of CdTe solar cells, to determine the impact of each step process during the cell manufacturing; this process consider deposition of CdS/CdTe as P1, thermal treatment to CdS (P2), thermal treatment of CdTe (P3) and p⁺ regions (Te or ZnTe) on CdTe (P4 and P5 respectively). All the I-V measures was made considering areas of 0.03cm², each back contact metal was isolated by laser scribing creating a square associated to the diameter of the back contact and a mask was used to cover the radiation incidence area on the substrate. The electrical parameters that are influenced by the diffusion and intermixing of each element can be observed on Figure 9. Electrical parameters, as short circuit current density J_{sc} , open circuit voltage V_{oc} , fill factor FF, efficiency η , ideality factor of a diode, series and shunt resistance R_s , R_{sh} are included.

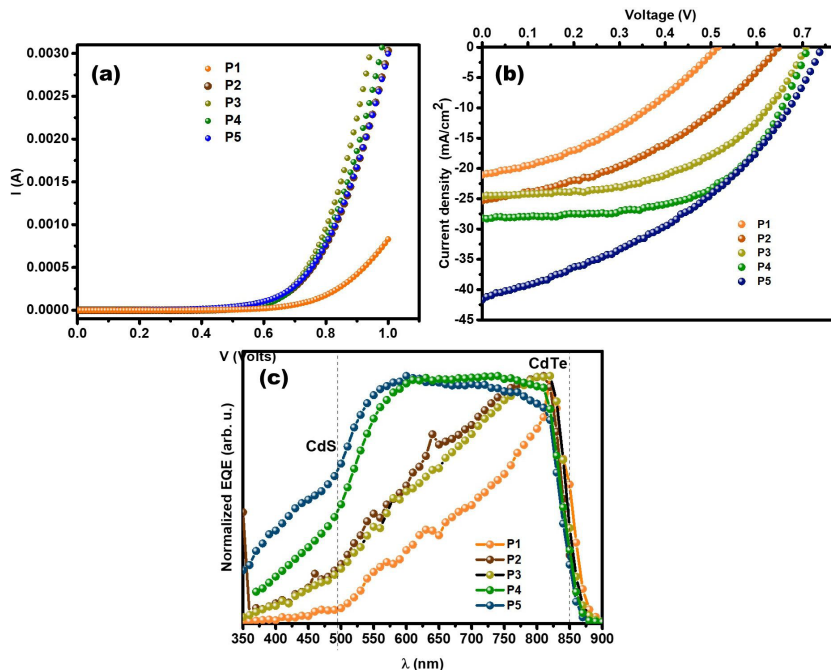


Figure 8. (a) Current vs voltage measure in dark condition, (b) Current density vs Voltage (J-V) measure under illumination and (c) Normalized Quantum Efficiency of CdS/CdTe solar cells.

Figure 8b shows a typically behavior for p-n junction without any thermal treatment using two different deposition techniques (see curve P1); where V_{OC} and FF values are low as is showed in Figure 9a. For all devices J_{SC} increase when CdS is thermally treated (see P2-P4 devices in Figure 9b), it is associate with an increase of photons conversion on electron as is observed on EQE curves in the region between 350nm to 550nm (see Figure 8c). An effective diffusion method in CdTe solar cells is treating thermally each thin film, as we can review along this work; as consequence of this result FF of P1, P2, P3 and P4 and increases due to the quality between junction created on CdTe solar cells are improved. A Te^+ region has been deposited on CdTe surface (P4 device) as part of the back contact achieving V_{OC} , FF, reducing potential barriers and decreasing de diode recombination; last result is confirmed by reduction of ideality factor diode (n) value, which was calculated by Cheung method (see Figure 9d)³⁶⁻³⁸, however P3 show a similar value considering a good thermal treatment of $CdCl_2$. The thermal treatment made to each thin film contribute to series and shunt resistance, as we can observe in Figure 9c. R_s values decrease while each thin film is treated and R_{sh} increase, where these values are related to contact resistivity and bulk resistivity, additionally R_s value for P5 device shows a high value, it has different possible causes to be increased: firstly, the movement of current through the emitter and base of the solar cell; secondly, the contact resistance between the metal contact and CdTe surface; and finally the resistance of the top and rear metal contacts, the last one is the most important for the solar cell P5 due to ZnTe region under deposited conditions generate a thin film increasing the series resistance as consequence the fill factor decrease as is observed in Figure 9a. On the other hand, EQE from P1, P2, P3, P4 and P5 devices allows

to observe the efficiency on photo-electron conversion. EQE comparison in Figure 8b shows the increasing collection in wavelength range from 350nm to 900nm specially at low wavelength as a result of the interdiffusion of elements such as Cd, Te, S or Cl into layer along the solar cell, we can expect that thin films get doped on each energy region associated to CdS and CdTe thin films (500nm and 800nm respectively). It means that at higher doping concentrations could produce a built-in potential increase. As a result, an added field is produced that helps to amplify the carrier collection. Additionally at higher electric field, the free carrier recombination reduces which results in the increase of open circuit voltage, and then the solar cell performance is improved³⁹. On the other hand, as we can see along the steps process of CdTe solar cells the interdiffusion allow us to expect an increase on the doping, that has an influence on the mobility and lifetime of the carriers that are generated. This increment has a correlation with a strong electrical field that could reduce recombination of carries separating these ones. Recording that each photon that strikes an ideal solar cell produces an electron-hole pair. External quantum efficiency (EQE) is the number of carriers contributed to the external load for each incident of photons. Then the photon generated carriers will be gathered through the contacts. The Figure 8c shows the EQE with respect to wavelength in the manuscript. It shows that EQE is higher in the wavelength region of 550nm to 830nm. That means the absorber material absorbs more photons in this wavelength range and absorption goes down beyond 850nm wavelength. Since, more photons are absorbed in this range, more electron-hole pairs are also generated in this range. Hence more carriers contribute to current, it means that photons with adequate energy could create useful electron-hole pairs that produce an enhance of J_{SC} ³⁹⁻⁴¹.

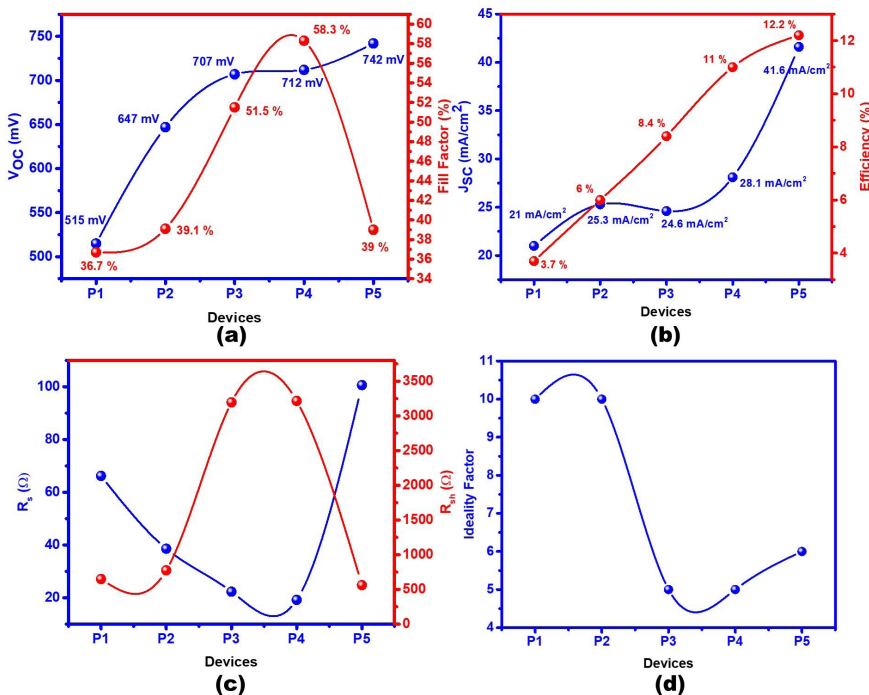


Figure 9. Electrical parameters of CdTe solar cells (a) V_{OC} , FF, (b) J_{SC} , η , (c) R_s , R_{sh} , and (d) ideality factor diode.

Moreover, it is important notice that solar cell P5 shows a high current density (see figure 8b and Figure 9b), however, this value is not completely correct because this indicates that is almost used all the photons from wavelength radiation creating electrical carriers; However, it is impossible considering the Schottky limit. To understand this effect SIMS analysis for ZnTe as part of the back contact allows observed that Zn as metal diffuses into CdTe solar cell reaching CdS/CdTe junctions (see Figure 7d and 7f), it means that Zn create a route to carries between front and back contacts producing a short circuit increasing the current measured. In addition, fill factor is affected obtaining a 39% value for diffusion of Zn because is possible the creation of compound between elements presents on each junction along CdTe solar cells. To understand the influence of ZnTe as part of the back contact in CdTe solar cell, SIMS and SEM measurements was used to analyze the presence of Zn along CdTe solar cells, considering the different morphologies deposited on CdTe surface that are associated to temperature, distance between powder source and substrate, and chamber deposition. For this reason, cell P5 was analyzed according to the Figure 10.

Solar cell P5 shows substantial differences between the deposited contacts, as can be seen in Figure 10, the cell has a different coloration from the center to the ends of the device, it means that ZnTe deposited on CdTe surface as well as Cu/Au metallic contact, the morphology, chemical composition of specific zones and photovoltaic conversion efficiencies in some representative metallic contacts were analyzed. The areas analyzed A_1 , A_2 and B_1 as well as contacts

A and B are shown in Figure 10. Point A and B referred to the metallic contacts of the center and right-side show Au, Cu and Te signals and atomic values of 51%, 8% and 40% respectively, it is observed that the presence of Au is bigger than Cu, which indicates that Cu begging diffuse faster than Au, as detailed in SIMS (see Figure 7f).

Point A_1 shows a shade along CdTe surface as is detailed in Figure 10. For this reason, the morphology was analyzed, and EDS color-coded elemental mapping was performed, considering that the shade region could be an oxidation or an excessive deposit of ZnTe. Figure 10 shows the Cd, Te and Zn signal elements that are statistically distributed near to the center contact, the elemental analysis shows that in the analyzed region there is 6.2% of Zn, 17.7% of Cd and in greater quantity it is found Te with 76.1%, this result is according to the semiconductor doping generating a better ohmic region which is observed on solar cell efficiency.

Region A_2 obtained from ZnTe deposit shows the distribution of the materials on CdTe surface where a very notable change in relation to point A_1 was observed. Morphology in region A_2 allows to see a saturation zones; the EDS color-coded elemental mapping carried out that the over-deposition generates regions rich in Cd and Te and poor Zn signal it means that Zn do not be evaporated or Zn traces are diffused into CdTe/CdS junctions, due to only 2.8% of Zn was detected on CdTe surface, while 14.6% Cd and 82.64% Te were detected, the last one could be oxidized generating a shadow appearance around the contacts. This deposition behavior could be attribute to ZnTe deposition temperature.

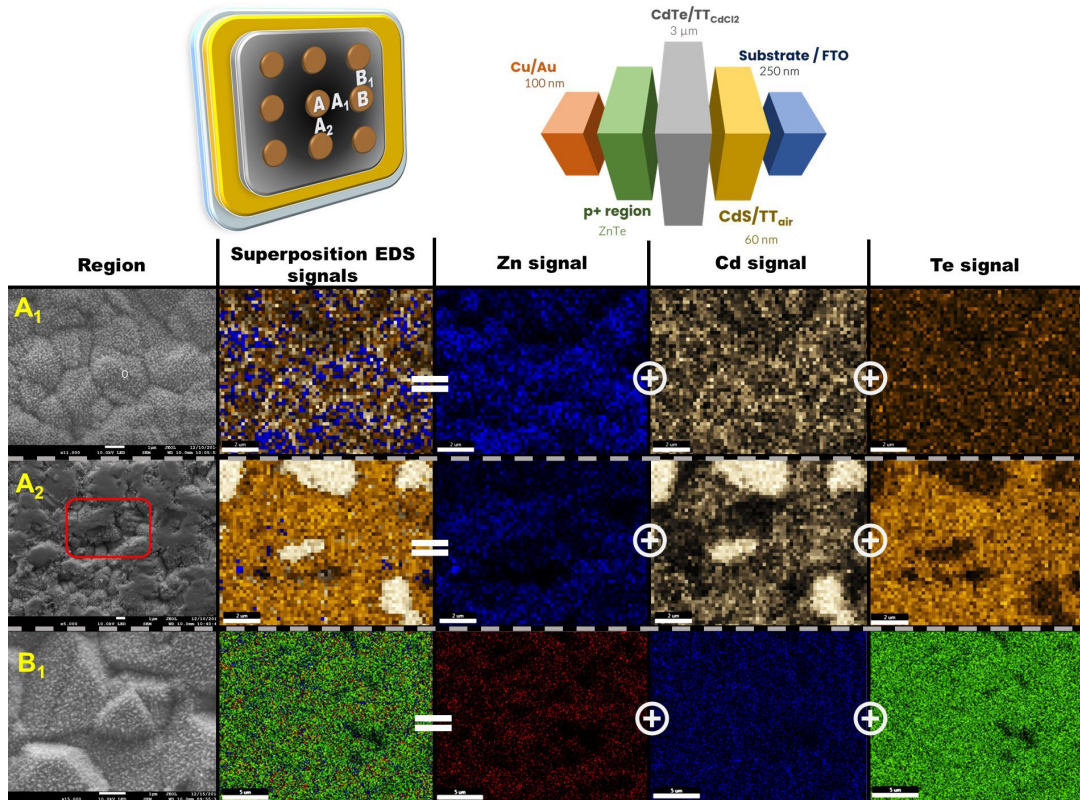


Figure 10. EDS color-coded elemental mapping for region A_1 , A_2 y B_1 of P5 solar cell.

Finally analyzing the morphology of point B₁ that is located to one side of the most efficient contact, it is possible to see a columnar morphology (Figure 10). In this region, a color mapping was performed again to observe the distribution of the elements, which revealed that both Zn, Cd and Te are found well distributed. The morphology and elemental analyze obtained suggest that the ZnTe deposit is not uniform throughout the deposit area, which implies variations in efficiency. Therefore, currents that are created on CdTe device could travel to the Zn metallic diffused along photovoltaic device contributing to the increase of the current, as consequence of this, will be required to search more routes to growth ZnTe on CdTe surface as part of the back contact.

To analyze the stability of solar cells according to Cu diffusion just we measured J-V for P3, P4 and P5 these has the complete solar cell process and p⁺ regions.

I-V electrical response of P3, P4 and P5 photovoltaic devices influenced by the time (24 months) are shows in Figure 11. The electrical parameters are reduced with respect to time. In Table 2 are reported the electrical parameters of the photovoltaic devices on detail. P3 photovoltaic device (see Figure 11a) shows the bigger degradation about of 50%; while P4 photovoltaic efficiency is reduced from 12% to 7.9% it means a degradation of 34%. Figure 11c shows the electrical degradation for P5 device, parameters such as V_{oc}, J_{sc}, FF and efficiency was not affected as much as in the P4 device used as part of the back contact, it means ZnTe deposited on CdTe surface is more functional as part of the metal contact.

We assume that using Te as part of the back contact V_{oc} and FF electrical parameters can be improved, however, ZnTe provides greater stability in the performance of CdTe photovoltaic solar cells along the time.

4. Conclusions

In this work CBD and CSVT systems was used for the successful fabrication of the thin films of CdS, CdTe, Te, ZnTe and CdCl₂ thermal treatments. Step by step analysis was used to understand the elements behavior along photovoltaic device. The fabricated films were analyzed with various physical characterization using SEM-EDS, SIMS, EDS color-coded elemental mapping, lineal EDS, and photovoltaic devices were analyzed by I-V, EQE. SEM-EDS and SIMS analysis showed that elements nature diffuses and intermixing between thin films junctions. Cd, S, Te and Zn diffusion and intermixing play an important role on electrical solar cell behavior. Cl, O, diffusion along CdTe solar cells contribute to the series and shunt resistance increasing electrical parameters and diffusion values were establish in this process. Additionally, was found that Cl is present along the solar cell on each step of manufacture. For CdTe solar cells with Te as part of back contact, the photovoltaic efficiency depends on Cu and Au diffusion values, if diffusion increase more than 150nm conflicts on carrier transport can be occurs; while ZnTe allow to reduce diffusion of Cu, however Zn diffusion create paths that produces shorts circuits creating a high current density but affecting fill factor of the device.

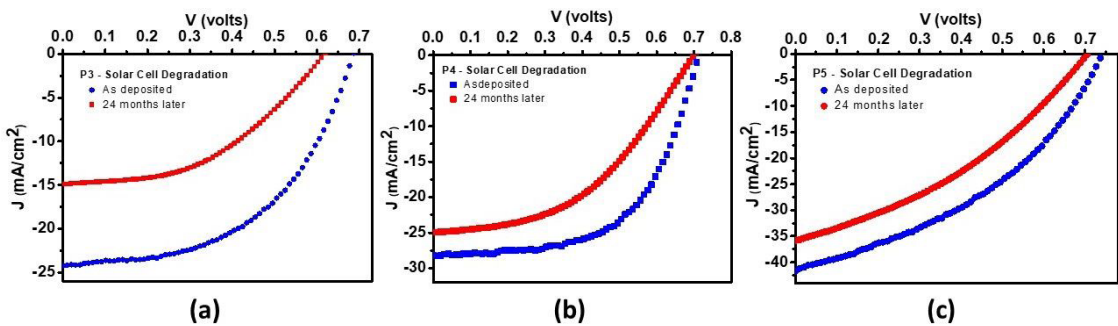


Figure 11. J-V measurements as deposited (blue line) and 24 months later (red line) for (a) P3, (b) P4, and (c) P5 devices.

Table 2. Electrical parameters of P3, P4 and P5 devices as deposited and 24 months later.

Solar Cell	V _{oc} (mV) ± 1 mV	J _{sc} (mA/cm ²) ± 3 mA/cm ²	FF (%) ± 0.6%	R _s (Ω) ± 0.1 Ω	R _{sh} (Ω) ± 0.1 Ω	n	η (%) ± 0.8%	Degradation (%)
P3 as deposited	707	24.6	51.5	122.8	3396.1	5	8.4	
P3 24 months later	617	14.8	45.7	103.5	1604.2	4.4	4.2	50
P4	729	28	60.6	93.5	4364.7	1.8	12.0	
P4 24 months later	699	25	45.4	157.2	2224.1	4.4	7.9	34
P5	742	41	39.5	773.4	3742.1	7.9	12.2	
P5 24 months later	705	36	35.9	819.7	2512.2	6.3	9.1	25

SIMS technique provide an important tool to observe each thin films interphases and performance in solar cells. To check the stability of the back contact metal on Te, ZnTe and Cu/Au devices, is determine that a nanostructure create a better region instead of a thin film between semiconductor/metal junction.

5. Acknowledgment

This work was supported by Instituto Politécnico Nacional, SIP-20231014, SIP-20231026, SIP-20231027, SIP-20230690 and CONAHCyT.

6. References

- Schneller T, Waser R, Kosec M, Payne D. Chemical solution deposition of functional oxide thin films [Internet]. Wien: Springer; 2013 [cited 2023 May 30]. Available from <https://link.springer.com/book/10.1007/978-3-211-99311-8>
- Kumar VN, Suriakarthik R, Shyju TS, Gopalakrishnan R. Deposition of CdS thin films by chemical bath and photochemical deposition methods and its characterization. *AIP Conf Proc*. 2013;1536:347-8. <http://dx.doi.org/10.1063/1.4810243>.
- Flores-Marquez JM, Albor-Aguilera ML, Matsumoto-Kuwabara Y, Gonzalez-Trujillo MA, Hernandez-Vasquez C, Mendoza-Perez R et al. Improving CdS/CdTe thin film solar cell efficiency by optimizing the physical properties of CdS with the application of thermal and chemical treatments. *Thin Solid Films*. 2015;582:124-7. <http://dx.doi.org/10.1016/j.tsf.2014.10.070>.
- Hernández-Calderón V, Vigil-Galán O, Pulgarín-Agudelo FA, Courel M, Arce-Plaza A, Cruz-Gandarilla F et al. Optimization of Cd_xZn_{1-x}S compound from CdS/ZnS bi-layers deposited by chemical bath deposition for thin film solar cells application. *Thin Solid Films*. 2019;676:100-7. <http://dx.doi.org/10.1016/j.tsf.2019.03.003>.
- Amin N, Yamada A, Konogai M. Effect of ZnTe and CdZnTe alloys at the back contact of 1- μ m-thick CdTe thin film solar cells. *Jpn J Appl Phys*. 2002;41:2834-41. <http://dx.doi.org/10.1143/JJAP.41.2834>.
- Gupta A, Parikh V, Compaan AD. High efficiency ultra-thin sputtered CdTe solar cells. *Sol Energy Mater Sol Cells*. 2006;90:2263-71. <http://dx.doi.org/10.1016/j.solmat.2006.02.029>.
- Abad WK, Maki SA, Alattar FIM. Fabrication and characterization of FTO/CdS/CdTe/Al solar cell. *AIP Conf Proc*. 2021;2372:170002. <http://dx.doi.org/10.1063/5.0066104>.
- Pandey SK, Tiwari U, Raman R, Prakash C, Krishna V, Dutta V et al. Growth of cubic and hexagonal CdTe thin films by pulsed laser deposition. *Thin Solid Films*. 2005;473:54-7. <http://dx.doi.org/10.1016/j.tsf.2004.06.157>.
- Arce-Plaza A, Andrade-Arvizu JA, Courel M, Alvarado JA, Ortega-López M. Study and application of colloidal systems films for obtaining CdTe+Te thin by spray pyrolysis. *J Anal Appl Pyrolysis*. 2017;124:285-9. <http://dx.doi.org/10.1016/j.jaap.2017.01.022>.
- Mathew X, Pantoja Enriquez J, Romeo A, Tiwari AN. CdTe/CdS solar cells on flexible substrates. *Sol Energy*. 2004;77:831-8. <http://dx.doi.org/10.1016/j.solener.2004.06.020>.
- Vigil-Galán O, Courel M, Cruz-Gandarilla F, Seuret-Jiménez D. CdTe:Bi films deposited by closed space vapor transport under variable pressure and doping levels: evidences of the possible formation of an intermediate band. *J Mater Sci Mater Electron*. 2016;27:6088-95. <http://dx.doi.org/10.1007/s10854-016-4534-1>.
- Vigil-Galán O, Marín E, Sastré Hernández J, Saucedo E, Ruiz CM, Contreras-Puente G et al. A study of the optical absorption in CdTe by photoacoustic spectroscopy. *J Mater Sci*. 2007;42:7176-9. <http://dx.doi.org/10.1007/s10853-006-1246-6>.
- Major JD, Proskuryakov YY, Durose K, Zoppi G, Forbes I. Control of grain size in sublimation-grow CdTe, and the improvement in performance of devices with systematically increased grain size. *Sol Energy Mater Sol Cells*. 2010;94:1107-12. <http://dx.doi.org/10.1016/j.solmat.2010.02.034>.
- Fritsche J, Schulmeyer T, Thiben A, Klein A, Jaegermann W. Interface modification of CdTe thin film solar cells by CdCl₂-activation. *Thin Solid Films*. 2015;431-432:267-71. [http://dx.doi.org/10.1016/S0040-6090\(03\)00269-4](http://dx.doi.org/10.1016/S0040-6090(03)00269-4).
- Huo X, Peng X, Liu W, Mo X, Chen G, Wang S et al. Comparison between the effects of CdCl₂ heat treatment on CdTe films prepared by RF magnetron sputtering and close spaced sublimation methods. *J Mater Sci Mater Electron*. 2013;24:2479-84. <http://dx.doi.org/10.1007/s10854-013-1121-6>.
- Moutinho HR, Al-Jassimm MM, Abulfotuh FA, Levi DH, Diplo PC, Dhere RG et al. Studies of recrystallization of CdTe thin films after CdCl₂ treatment. In: 26th IEEE Photovoltaic Specialists Conference; 1997 Sep/Oct 29-3; Anaheim. Proceedings. New York: IEEE; 1997. p. 431-434. <http://dx.doi.org/10.1109/PVSC.1997.654120>.
- Green MA, Dunlop ED, Hohl-Ebinger J, Yoshita M, Kopidakis N, Ho-Baillie AWY. Solar cell efficiency tables (version 55). *Prog Photovolt Res Appl*. 2020;28:3-15. <http://dx.doi.org/10.1002/pip.3228>.
- Shockley W, Queisser HJ. Detailed balance limit of efficiency of p-n Junction Solar Cells. *J Appl Phys*. 1961;32:510-9. <http://dx.doi.org/10.1063/1.1736034>.
- Hernández Vásquez C, Albor Aguilera ML, González Trujillo MA, Flores Márquez JM, Jiménez Olarte D, Gallardo Hernández S et al. Enhancement of CdS/CdTe solar cells by the interbuilding of a nanostructured Te rich layer. *Mater Res Express*. 2017;4:0864043. <http://dx.doi.org/10.1088/2053-1591/aa7d88>.
- Bätzner DL, Wendt R, Romeo A, Zogg H, Tiwari AN. A study of the back contacts on CdTe/CdS solar cells. *Thin Solid Films*. 2000;361-362:463-7. [http://dx.doi.org/10.1016/S0040-6090\(99\)00842-1](http://dx.doi.org/10.1016/S0040-6090(99)00842-1).
- Uličná S, Isherwood PJM, Kaminski PM, Walls JM, Li J, Wolden CA. Development of ZnTe as a back contact material for thin film cadmium telluride solar cells. *Vacuum*. 2017;139:159-63. <http://dx.doi.org/10.1016/j.vacuum.2017.01.001>.
- Wolden CA, Abbas A, Li J, Diercks DR, Meysing DM, Ohno TR et al. The roles of ZnTe buffer layers on CdTe solar cell performance. *Sol Energy Mater Sol Cells*. 2016;147:203-10. <http://dx.doi.org/10.1016/j.solmat.2015.12.019>.
- Bista SS, Li DB, Lei C, Grice C, Awni RA, Song Z et al. ZnTe back buffer layer to enhance the efficiency of CdS/CdTe solar cells. In: 2019 IEEE 46th Photovoltaic Specialists Conference (PVSC); 2019 Jun 16-21; Chicago. Proceedings. New York: IEEE; 2019. p. 0499-502. <http://dx.doi.org/10.1109/PVSC40753.2019.8981157>.
- Albor Aguilera ML, Flores Márquez JM, Remolina-Millán A, Kuwabara YM, González Trujillo MA, Hernández Vásquez C et al. Cu doping concentration effect on the physical properties of CdS thin films obtained by the CBD technique. *Mater Res Express*. 2017;4:086410. <http://dx.doi.org/10.1088/2053-1591/aa810c>.
- Ortega-Cardenas JA, Albor-Aguilera ML, Hernandez-Vasquez C, Flores-Marquez JM, Rueda-Morales G, Rangel-Kuoppa VT et al. Impact of different thermal treatments on ZnS physical properties and their performance in CdTe solar cells. *Mater Res Express*. 2019;6:08646. <http://dx.doi.org/10.1088/2053-1591/ab1d38>.
- Galarza-Gutierrez U, Albor-Aguilera ML, Gonzalez-Trujillo MA, Hernandez-Vasquez C, Ortega-Cardenas JA, Flores Marquez JM et al. Incorporation of an efficient β -In₂S₃ thin film as window material into CdTe photovoltaic devices. *Mater Res Express*. 2019;6:125510. <http://dx.doi.org/10.1088/2053-1591/ab5508>.

27. Islam MA, Haque F, Rahman KS, Dhar N, Hossain MS, Sulaiman Y et al. Effect of oxidation on structural, optical and electrical properties CdS thin films grown by sputtering. *Optik*. 2015;126:3177-80. <http://dx.doi.org/10.1016/j.ijleo.2015.07.078>.
28. Duenow JN, Dhare RG, Moutinho HR, To B, Pankow JW, Kuciauskas D et al. CdS_xTe_{1-x} alloying in CdS/CdTe solar cells. *MRS Online Proc Libr*. 2011;1324:1403. <http://dx.doi.org/10.1557/opl.2011.1151>.
29. Mathew X, Cruz JS, Coronado DR, Millan AR, Segura GC, Morales ER et al. CdS thin film post-annealing and Te-S interdiffusion in a CdTe/CdS solar cell. *Sol Energy*. 2012;86:1023-8. <http://dx.doi.org/10.1016/j.solener.2011.06.024>.
30. Hernandez Vasquez C, Albor Aguilera ML, González Trujillo MA, Flores Márquez JM, Galarza Gutiérrez U, Aguilar Hernandez JR et al. Study of CdTe recrystallization by hydrated-CdCl₂ thermal treatment. *Rev Mex Fis*. 2017 [cited 2023 May 30];63(5):469-73. https://www.scielo.org.mx/scielo.php?pid=S0035-001X2017000500469&script=sci_arttext&tlng=en.
31. Islam MA, Haque F, Rahman KS, Dhar N, Hossain MS, Sulaiman Y et al. Effect of oxidation on structural, optical and electrical properties of CdS thin films grown by sputtering. *Optik*. 2015;126:3177-80. <http://dx.doi.org/10.1016/j.ijleo.2015.07.078>.
32. Lisco F, Kaminski PM, Abbas A, Bass K, Bowers JW, Claudio G et al. The structural properties of CdS deposited by chemical bath deposition and pulsed direct current magnetron sputtering. *Thin Solid Films*. 2015;582:323-7. <http://dx.doi.org/10.1016/j.tsf.2014.11.062>.
33. Alexander JN, Higashiya S, Caskey D Jr, Efstathiadis H, Haldar P. Deposition and characterization of cadmium sulfide (CdS) by chemical bath deposition using an alternative chemistry cadmium precursor. *Sol Energy Mater Sol Cells*. 2014;125:47-53. <http://dx.doi.org/10.1016/j.solmat.2014.02.017>.
34. Fritsche J, Gunst S, Golusda E, Lejard MC, Thißen A, Mayer T et al. Surface analysis of CdTe thin film solar cells. *Thin Solid Films*. 2001;387:161-4. [http://dx.doi.org/10.1016/S0040-6090\(00\)01851-4](http://dx.doi.org/10.1016/S0040-6090(00)01851-4).
35. Hofmann S. From depth resolution to depth resolution function: refinement of the concept for delta layers and multilayers. *Surf Interface Anal*. 1999;27:825-34. [http://dx.doi.org/10.1002/\(SICI\)1096-9918\(199909\)27:9<825::AID-SIA638>3.0.CO;2-D](http://dx.doi.org/10.1002/(SICI)1096-9918(199909)27:9<825::AID-SIA638>3.0.CO;2-D).
36. Rangel-Kuoppa VT, Albor-Aguilera ML, Hernández-Vásquez C, Flores-Márquez JM, González-Trujillo MA, Contreras-Puente GS. Shunt resistance and saturation current determination in CdTe and CIGS solar cells: I. A new theoretical procedure and comparison with other methodologies. *Semicond Sci Technol*. 2018;33:045007. <http://dx.doi.org/10.1088/1361-6641/aab017>.
37. Rangel-Kuoppa VT, Albor-Aguilera ML, Hernández-Vásquez C, Flores-Márquez JM, Jiménez-Olarte D, Sastré-Hernández J et al. Shunt resistance and saturation current determination in CdTe and CIGS solar cells: II. Application to experimental IV measurements and comparison with other methods. *Semicond Sci Technol*. 2018;33:045008. <http://dx.doi.org/10.1088/1361-6641/aab018>.
38. Cheung SK, Cheung NW. Extraction of Schottky diode parameters from forward current-voltage. *Appl Phys Lett*. 1986;49:85-7. <http://dx.doi.org/10.1063/1.97359>.
39. Sameera JN, Jhuma FA, Rashid MJ. Numerical approach to optimizing the doping concentration of the absorber layer to enhance the performance of a CdTe solar cell. *Semicond Sci Technol*. 2020;36(1):015022. <http://dx.doi.org/10.1088/1361-6641/abca0e>.
40. Dharmadasa IM, Bunning JD, Samantilleke AP, Shen T. Effects of multi-defects at metal/semiconductor interfaces on electrical properties and their influence on stability and lifetime of thin film solar cells. *Sol Energy Mater Sol Cells*. 2005;86:373-84. <http://dx.doi.org/10.1016/j.solmat.2004.08.009>.
41. Echendu OK, Fauzi F, Weerasinghe AR, Dharmadasa IM. High short-circuit current density CdTe solar cells using all-electrodeposited semiconductor. *Thin Solid Films*. 2014;556:529-34. <http://dx.doi.org/10.1016/j.tsf.2014.01.071>.